Photo-Thermal Synergistic CO_2 Hydrogenation towards CO over PtRh Bimetal-Decorated GaN Nanowires/Si

Jinglin Li[1+], Bowen Sheng[2+], Liang Qiu[1+], Jiajia Yang[2], Ping Wang[2]*, Yixin Li[1], Tianqi Yu[1], Hu Pan[1], Ying Li[1], Muhan Li[1], Lei Zhu[1]*, Xinqiang Wang[2,3,4]*, Zhen Huang[1], Baowen Zhou[1]*.

1. Key Laboratory for Power Machinery and Engineering of Ministry of Education, Research Center for Renewable Synthetic Fuel, School of Mechanical Engineering, Shanghai Jiao Tong University, 800 Dongchuan Road, Shanghai 200240, China.
2. State Key Laboratory of Artificial Microstructure and Mesoscopic Physics, School of Physics, Nano-Optoelectronics Frontier Center of Ministry of Education (NFC-MOE), Peking University, Beijing 10087, China.
3. Peking University Yangtze Delta Institute of Optoelectronics, Nantong, Jiangsu 226010, China.
4. Collaborative Innovation Center of Quantum Matter, School of Physics, Peking University, Beijing 100871, China.

* Corresponding authors Email: pingwang@pku.edu.cn; tonnyzhulei@sjtu.edu.cn; wangshi@pku.edu.cn; zhoubw@sjtu.edu.cn

+ These authors contributed equally to this work.

Table S1 The measured amounts of Pt and Rh in the optimized PtRh NPs/GaN NWs/Si.

Pt ($\mu mol \cdot cm^{-2}$)	Rh ($\mu mol \cdot cm^{-2}$)	Total ($\mu mol \cdot cm^{-2}$)
0.05	0.06	0.11

Table S2 The summary of the activity of light-driven CO_2 hydrogenation toward CO over various catalysts.

Catalyst	Reaction conditions	CO rate ($mol \cdot g_{cat}^{-1} \cdot h^{-1}$)	Selectivity of CO (%)	TOF (h^{-1})	Ref.
PtRh/GaN NWs/Si	CO_2:H_2=12:1, (1 bar) 300W Xe lamp, 5.3 $W \cdot cm^{-2}$	11.7	98.5	26,486	This work
Co@C-700	CO_2:H_2=1:1, (1 bar) 300W Xe lamp, 3 $W \cdot cm^{-2}$	0.54	92.6	-	1
Co@CoN&C	CO_2:H_2=1:1, (0.55 bar) 300W Xe lamp	0.13	91.1	-	2
Ni_3N Nanosheets	CO_2:H_2=20:1, (1 bar) 300W Xe lamp, 3.006 $W \cdot cm^{-2}$	1.21	99	-	3
K+-Co-C	CO_2:H_2=1:1, (1 bar) 300W Xe lamp, 2.8 $W \cdot cm^{-2}$	0.76	99.8	16,740	4
Ru/Mo_2TiC_2	CO_2:H_2:N_2=1:1:2, (1 bar) 300W Xe lamp, 3.8 $W \cdot cm^{-2}$	0.084	99	-	5

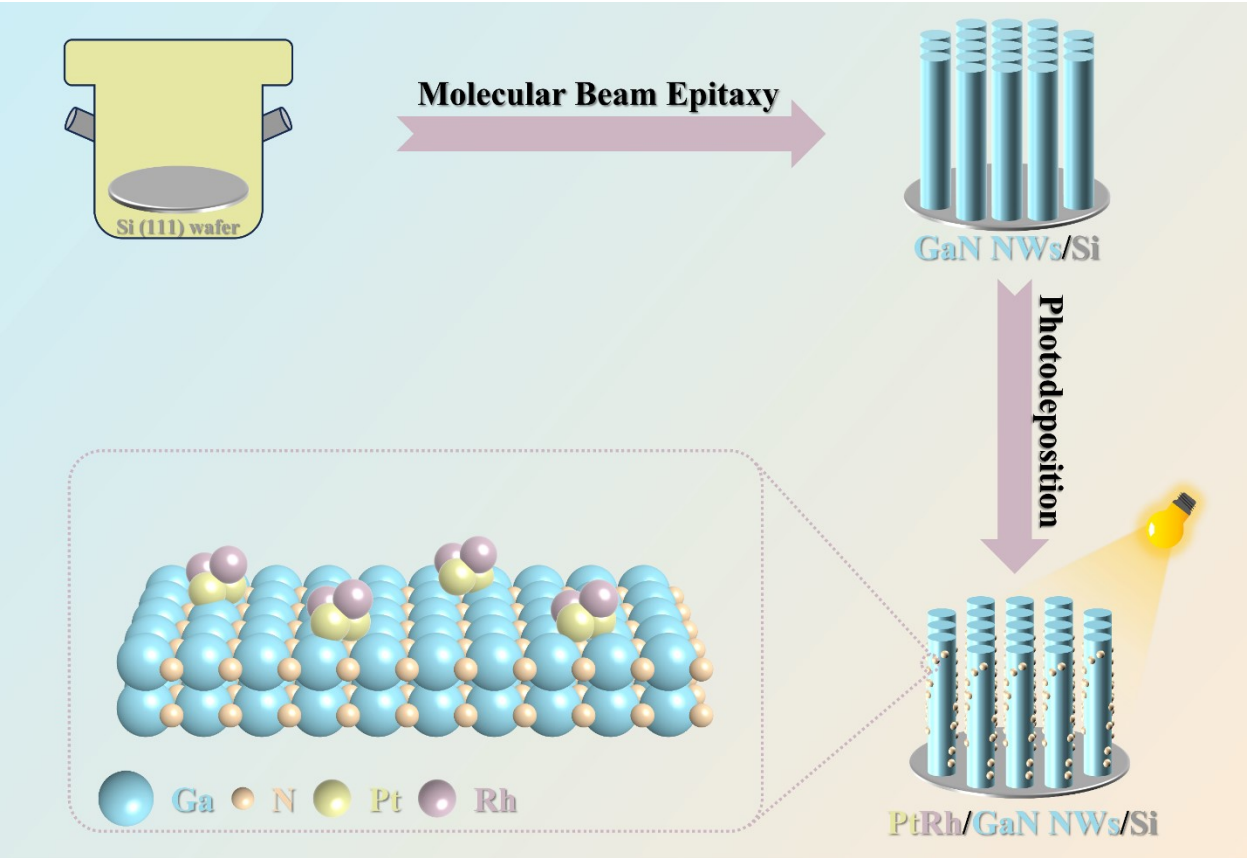

Fig. S1. Schematic diagram for assembling PtRh/GaN NWs/Si by coupling molecular beam epitaxy with photo-deposition.

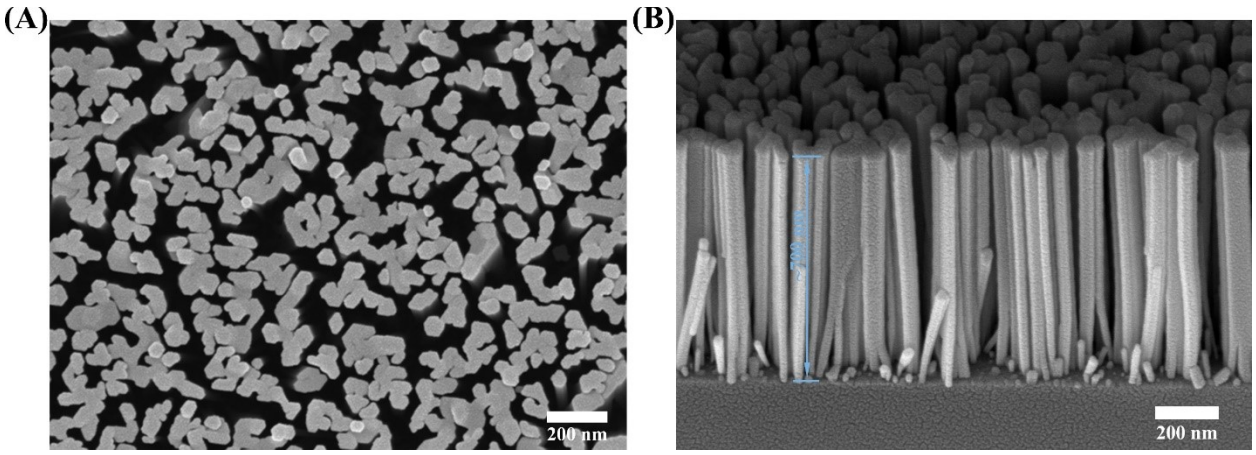

Fig. S2. (A) Top view and (B) side view of SEM images of GaN NWs/Si.

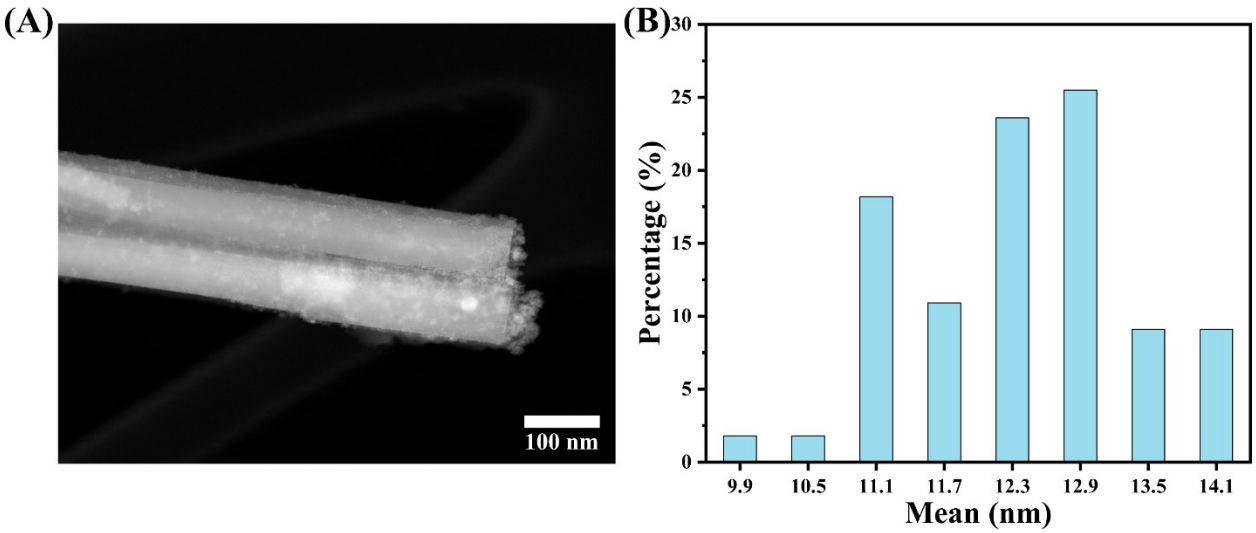

Fig. S3. (A) HADDF-STEM image and (B) the diameters distribution of PtRh/GaN NWs/Si with the PtRh loading content of 0.11 μmol·cm^{-2}.

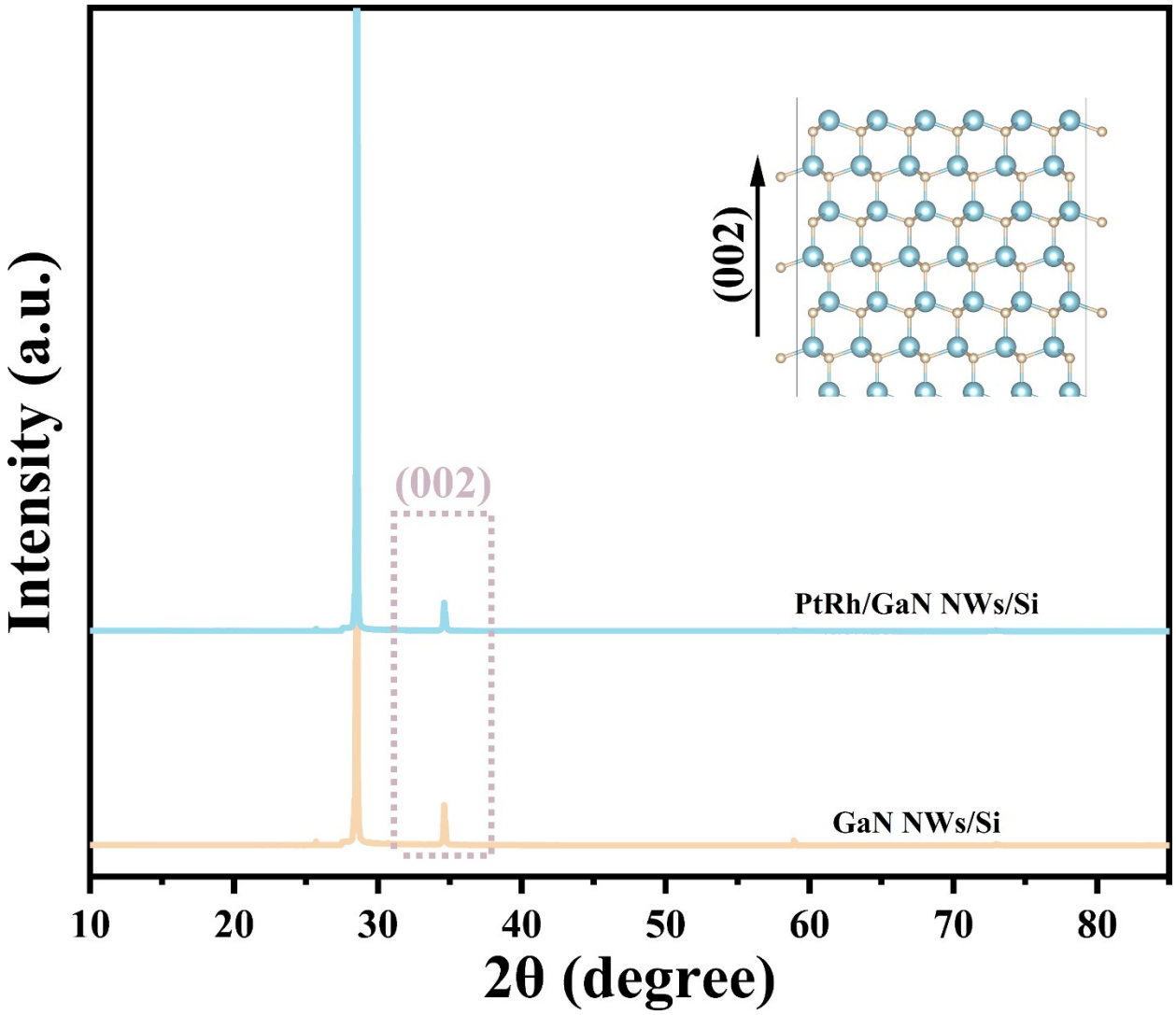

Fig. S4. XRD patterns of GaN NWs, and PtRh/GaN NWs supported by Si wafer, respectively.

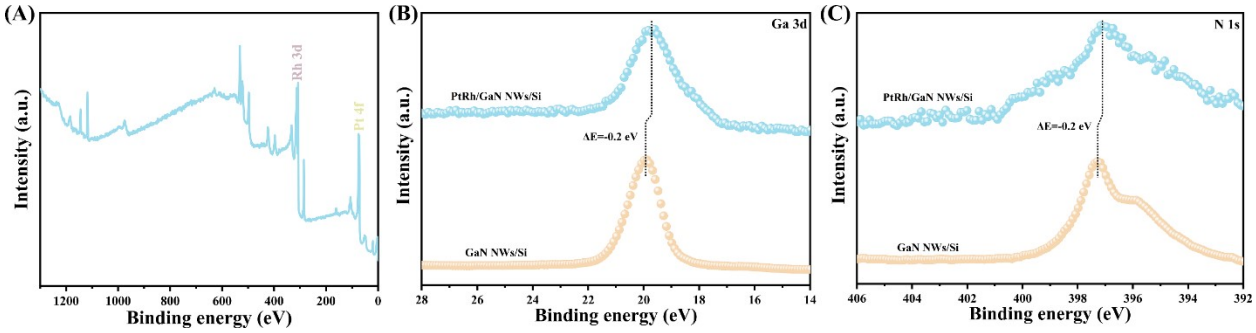

Fig. S5. XPS spectra of PtRh/GaN NWs/Si. (a) XPS survey, (b) Ga 3d, and (c) N 1s.

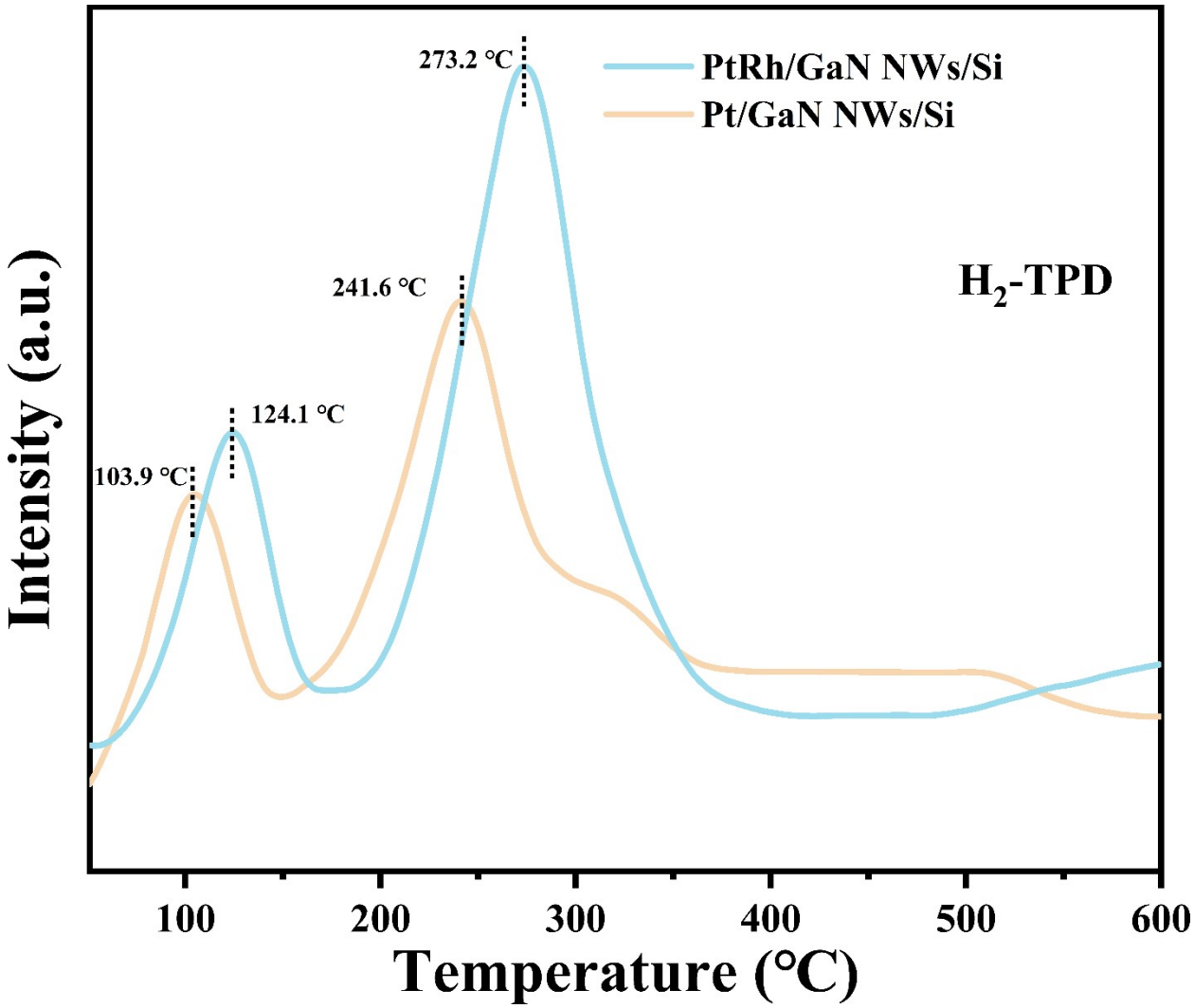

Fig. S6. H_2-TPD spectra of Pt/GaN NWs/Si and PtRh/GaN NWs/Si.

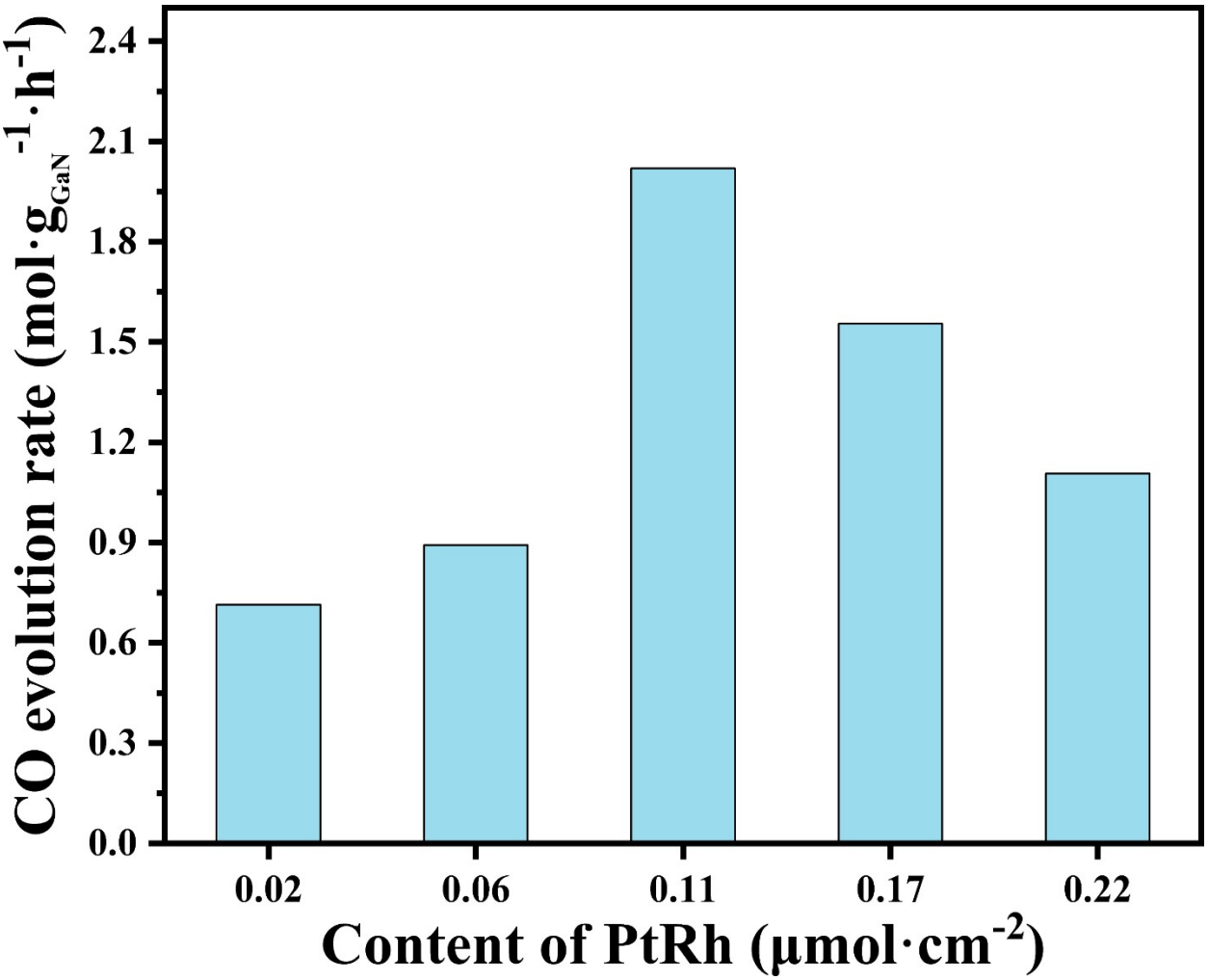

Fig. S7. Influence of the loading amount of PtRh on CO evolution rate over PtRh/GaN NWs/Si. Light intensity: 4.3 W·cm^{-2}; catalyst area: ~0.5 cm^{-2}; Rh:(Rh + Pt) = 0.55; CO_2:H_2 = 3:1.

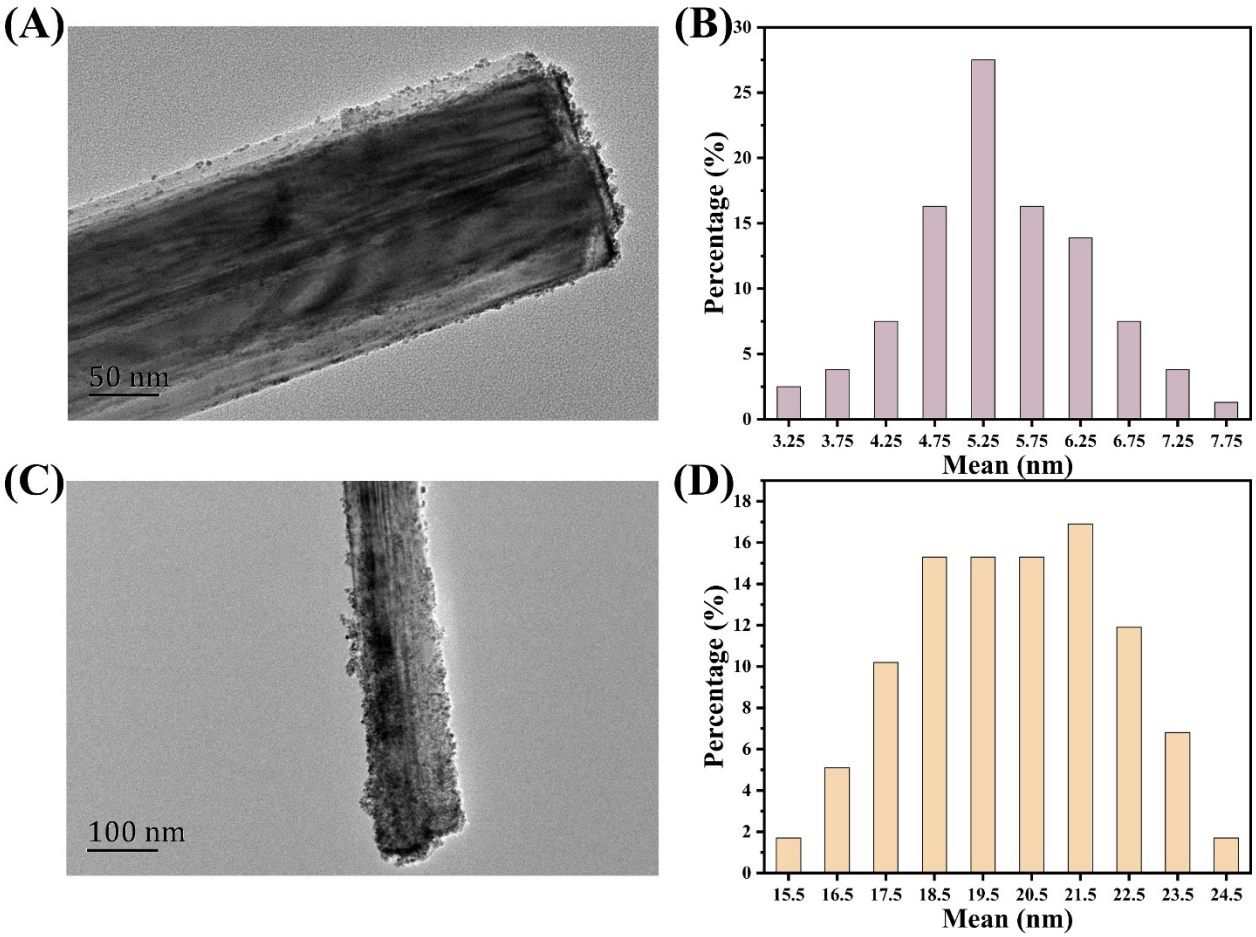

Fig. S8. TEM images of PtRh/GaN NWs/Si with the PtRh loading content of (A) 0.02 and (C) 0.22 μmol·cm^{-2}. The diameters distribution of PtRh NPs over GaN NWs/Si surface with the PtRh loading content of (B) 0.02 and (D) 0.22 μmol·cm^{-2}.

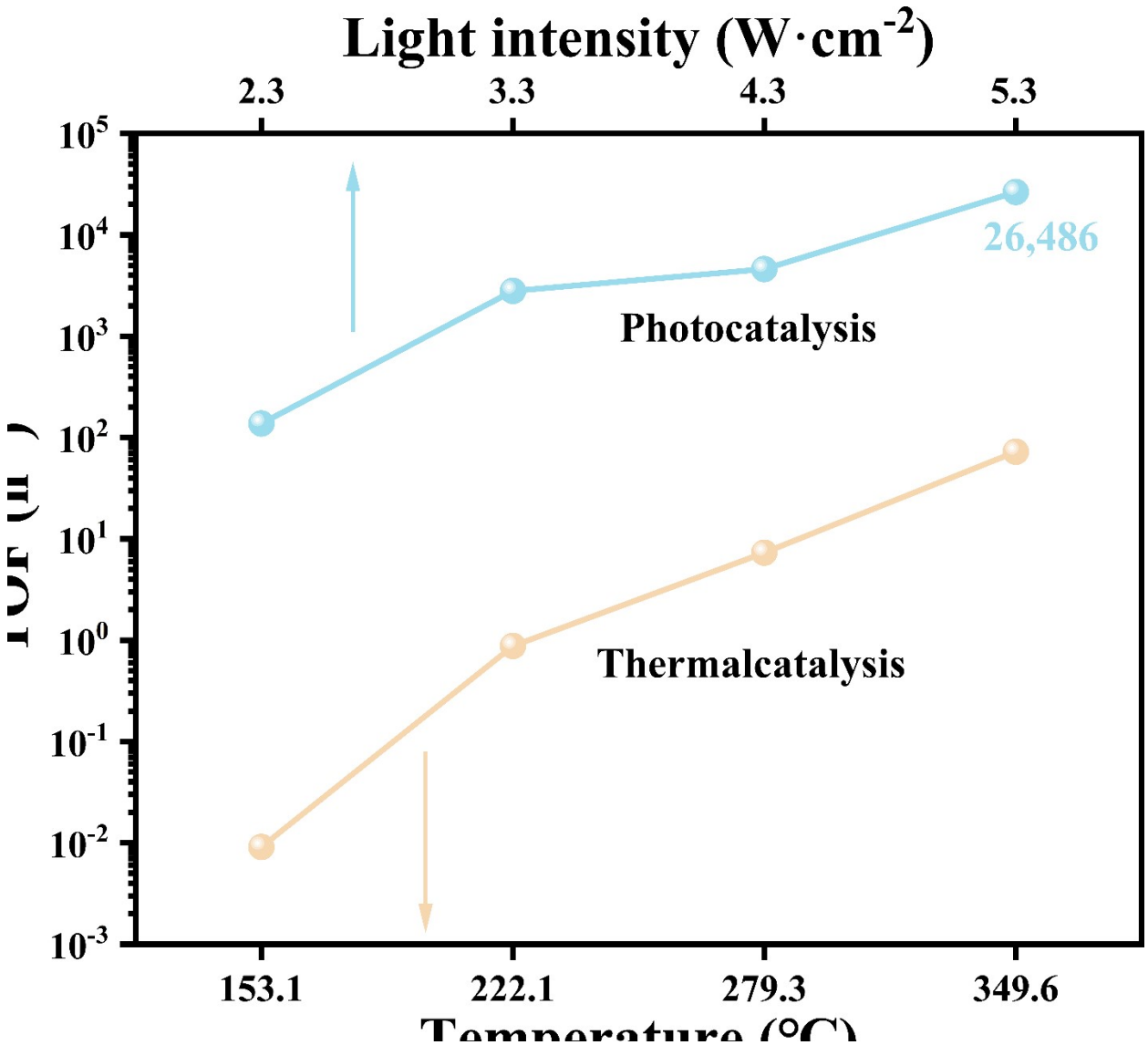

Fig. S9. TOF over PtRh/GaN NWs/Si under dark and concentrated light-illuminating conditions at different temperatures.

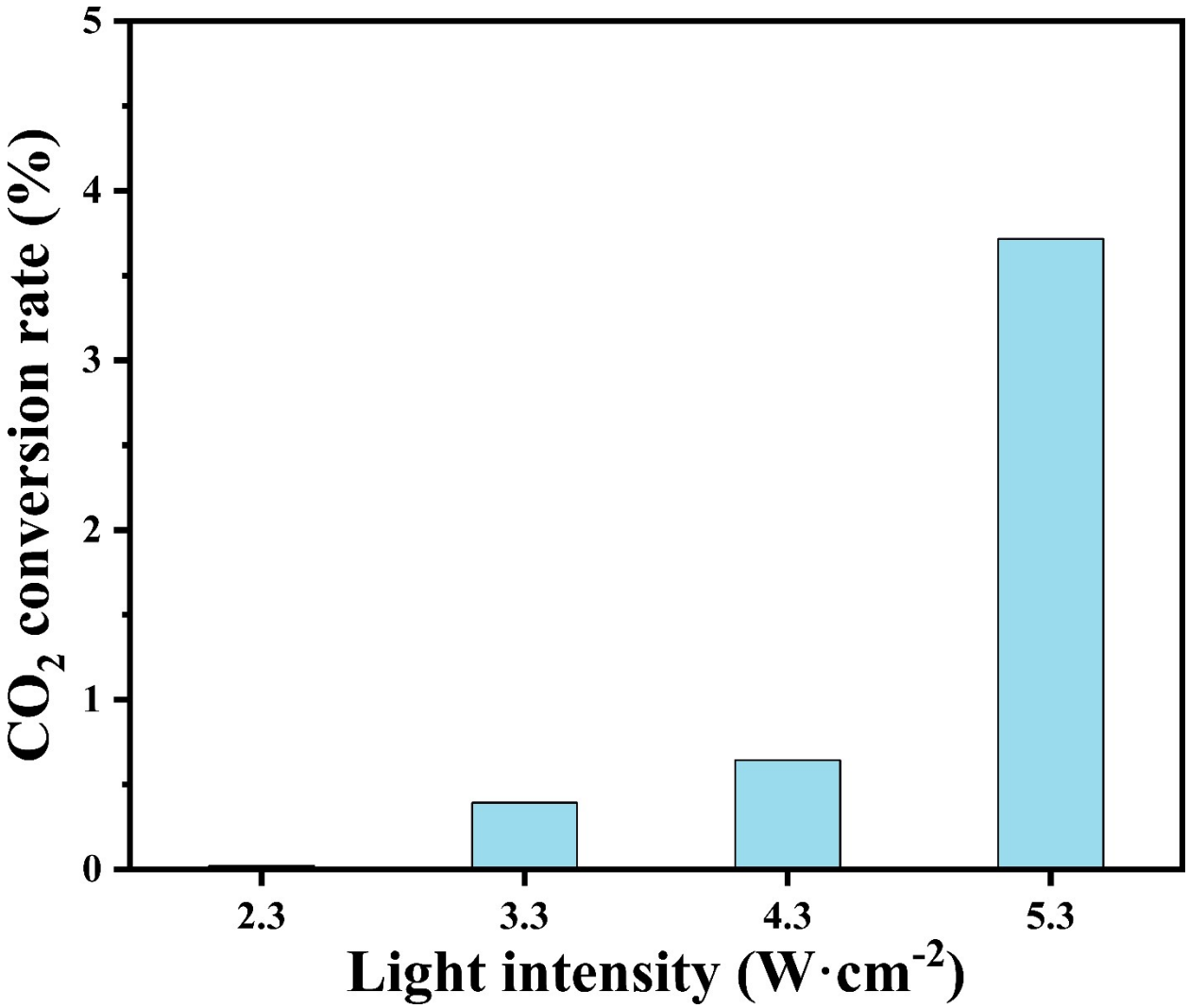

Fig. S10. CO_2 conversion rate over PtRh/GaN NWs/Si under concentrated light-illuminating conditions with different light intensities. Catalyst area: ~0.5 cm^{-2}; Rh:(Rh + Pt) = 0.55; PtRh: 0.11 μmol·cm^{-2}; CO_2:H_2 = 12:1, reaction time: 0.5 h.

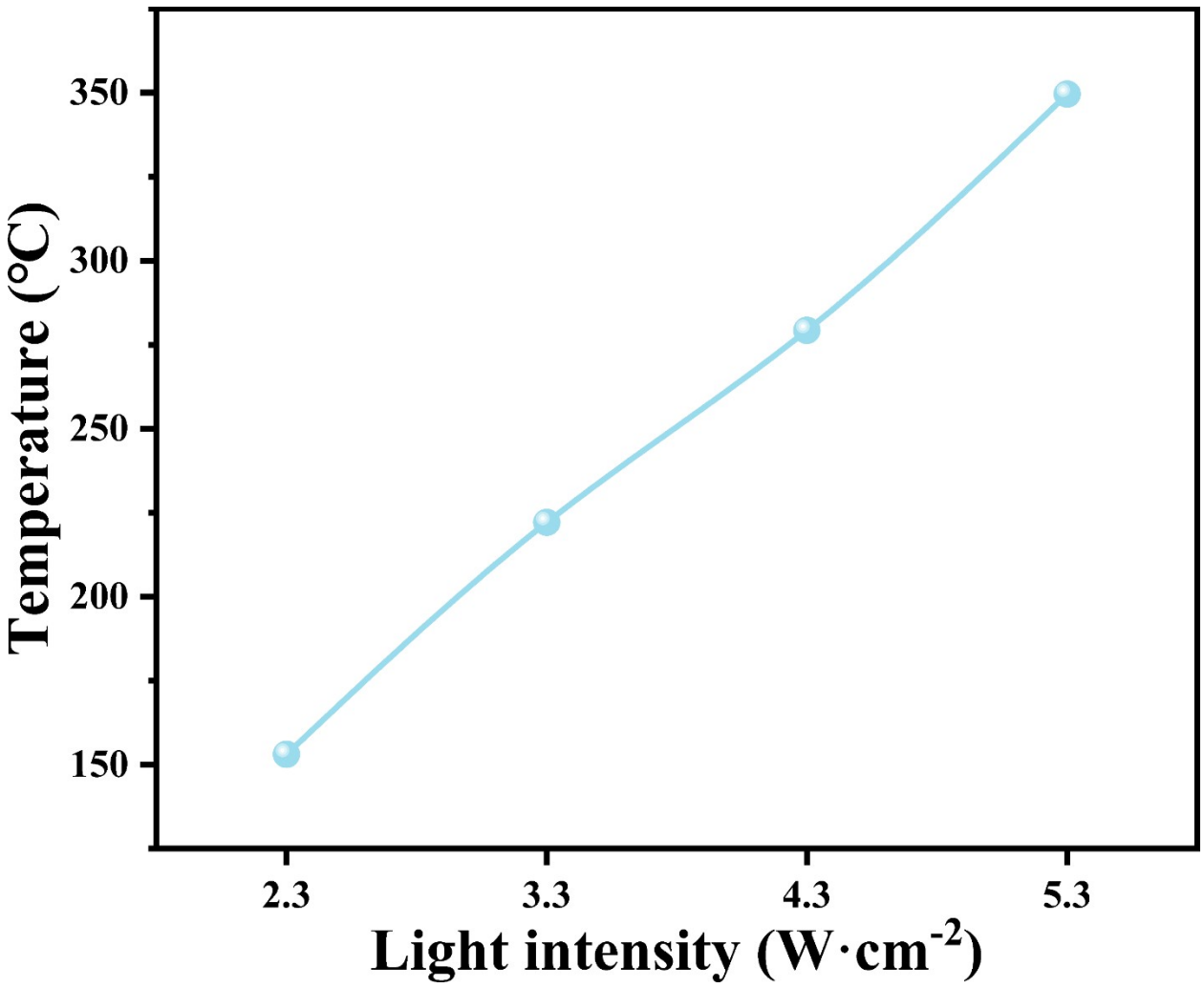

Fig. S11. Surface temperature of PtRh/GaN NWs/Si under various light intensities.

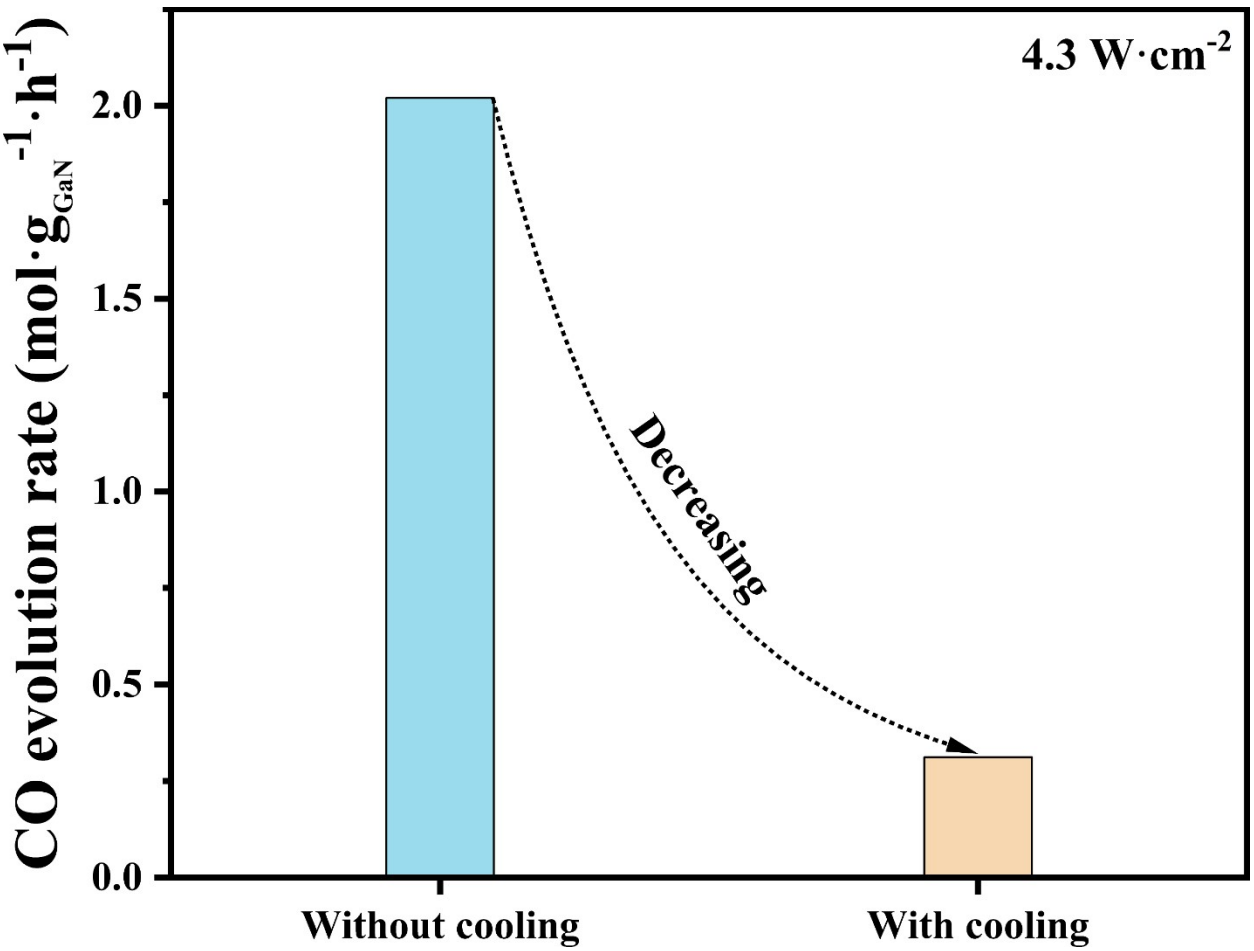

Fig. S12. CO evolution rate over PtRh/GaN NWs/Si with/without cooling. Light intensity: 4.3 $W \cdot cm^{-2}$; catalyst area: ~0.5 cm^{-2}; Rh:(Rh + Pt) = 0.55; PtRh: 0.11 $\mu mol \cdot cm^{-2}$; CO_2:H_2 = 12:1.

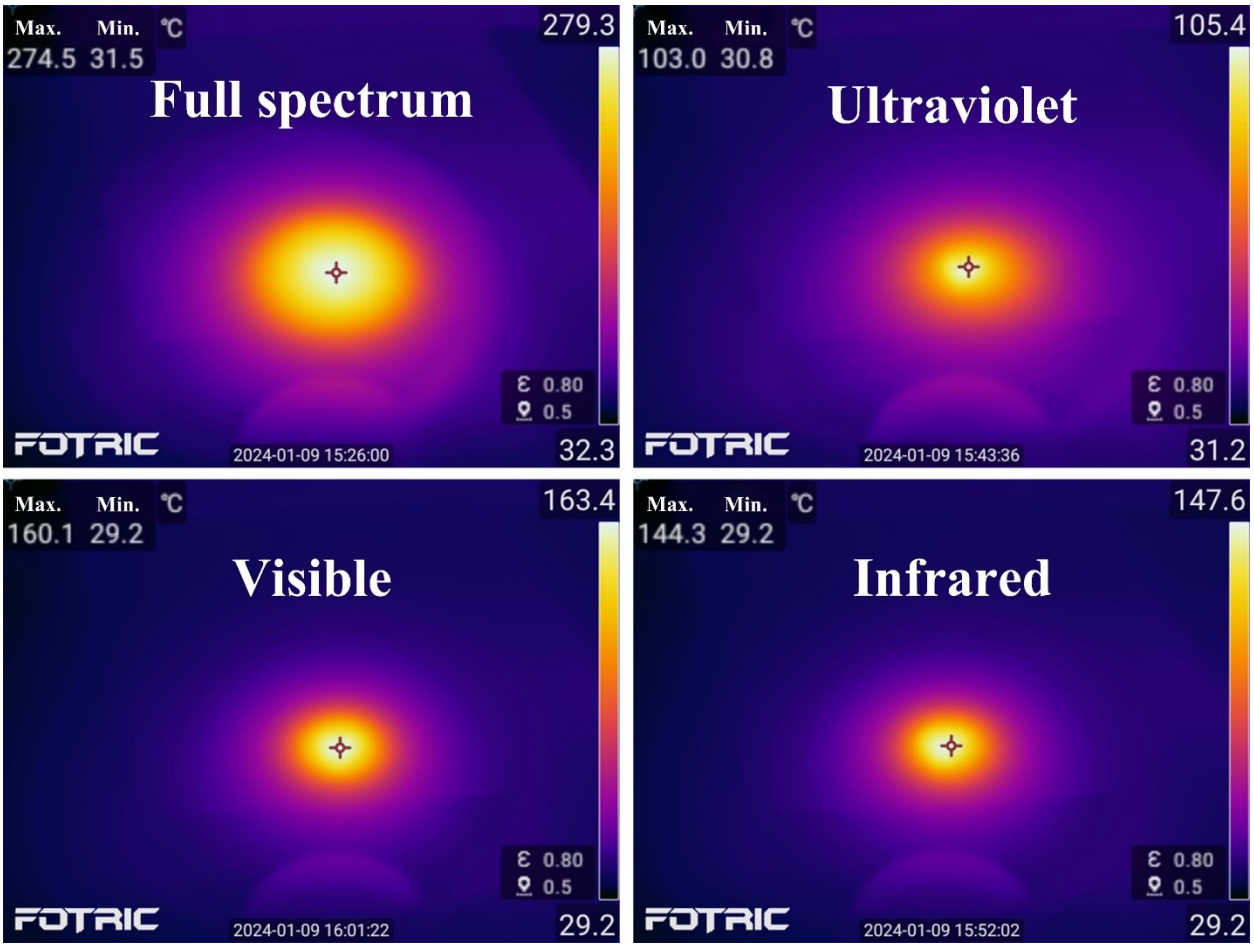

Fig. S13. Infrared thermal images over PtRh/GaN NWs/Si surface under light irradiation in different spectral ranges (full spectra, ultraviolet, visible, and infrared).

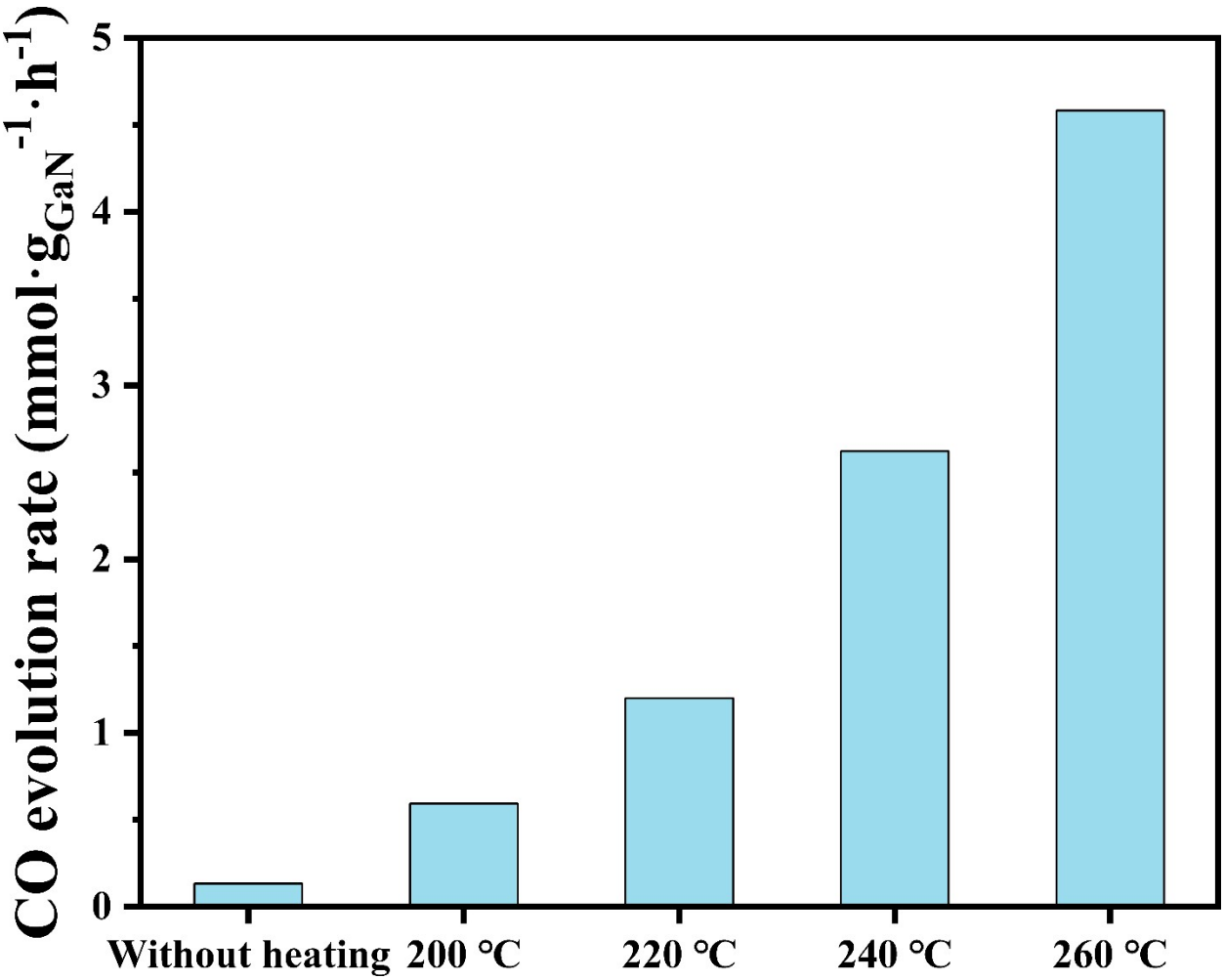

Fig. S14. The dependence of CO activity on temperature under ultraviolet light illumination. Light intensity: 2.1 W·cm^{-2}; catalyst area: ~0.5 cm^{-2}; Rh:(Rh + Pt) = 0.55; PtRh: 0.11 μmol·cm^{-2}; CO_2:H_2 = 12:1.

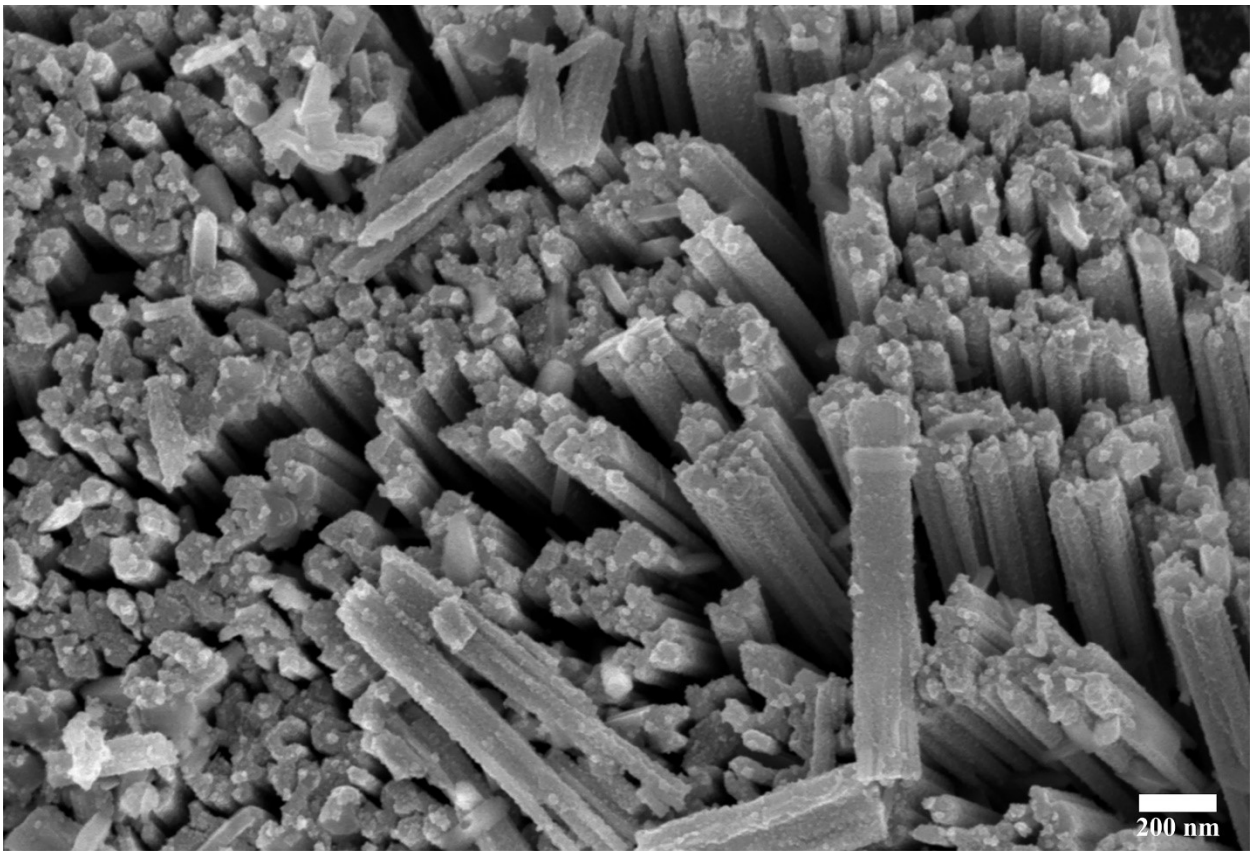

Fig. S15. (A) SEM image of PtRh/GaN NWs/Si after 16 h of durability testing.

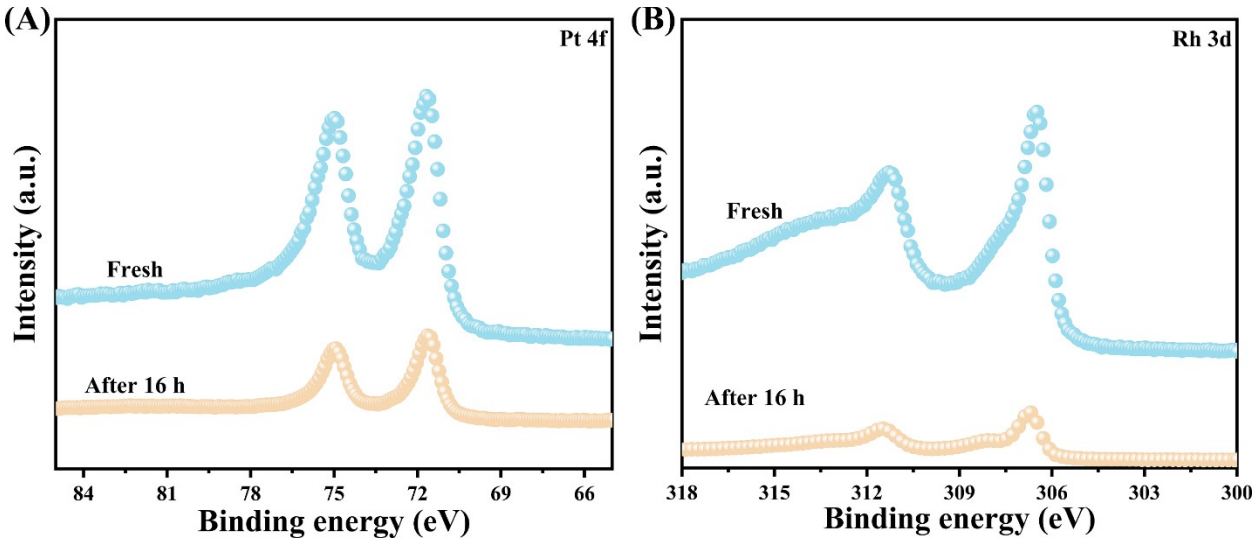

Fig. S16. XPS spectra of PtRh/GaN NWs/Si (fresh and after 16 h of durability testing. (A) Pt 4f. (B) Rh 3d.

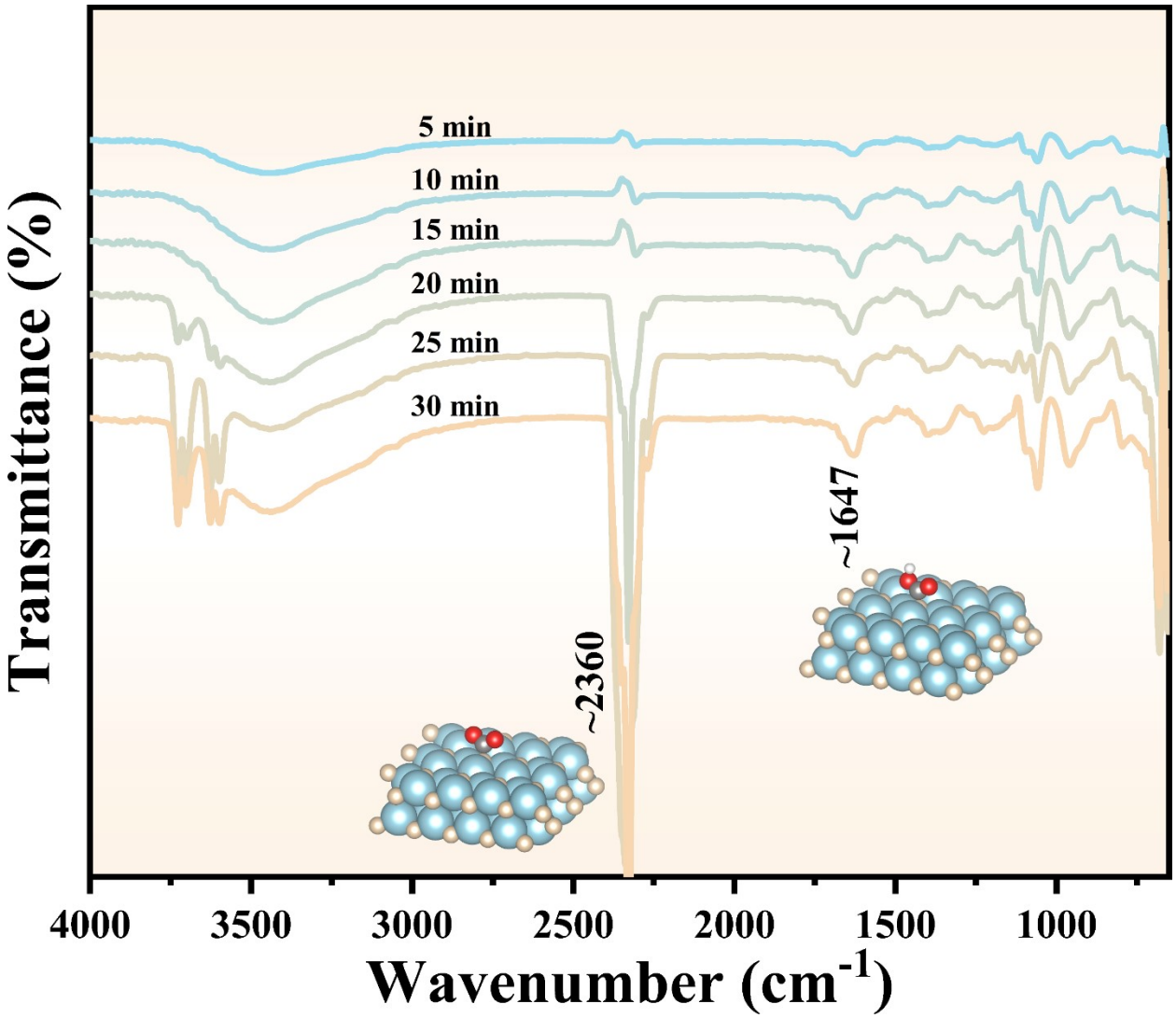

Fig. S17. *Operando* DRIFT spectra of CO_2 hydrogenation over PtRh/GaN NWs/Si under dark conditions at 280 °C. Ga, blue; N, orange; C, gray; O, red; and H, white.

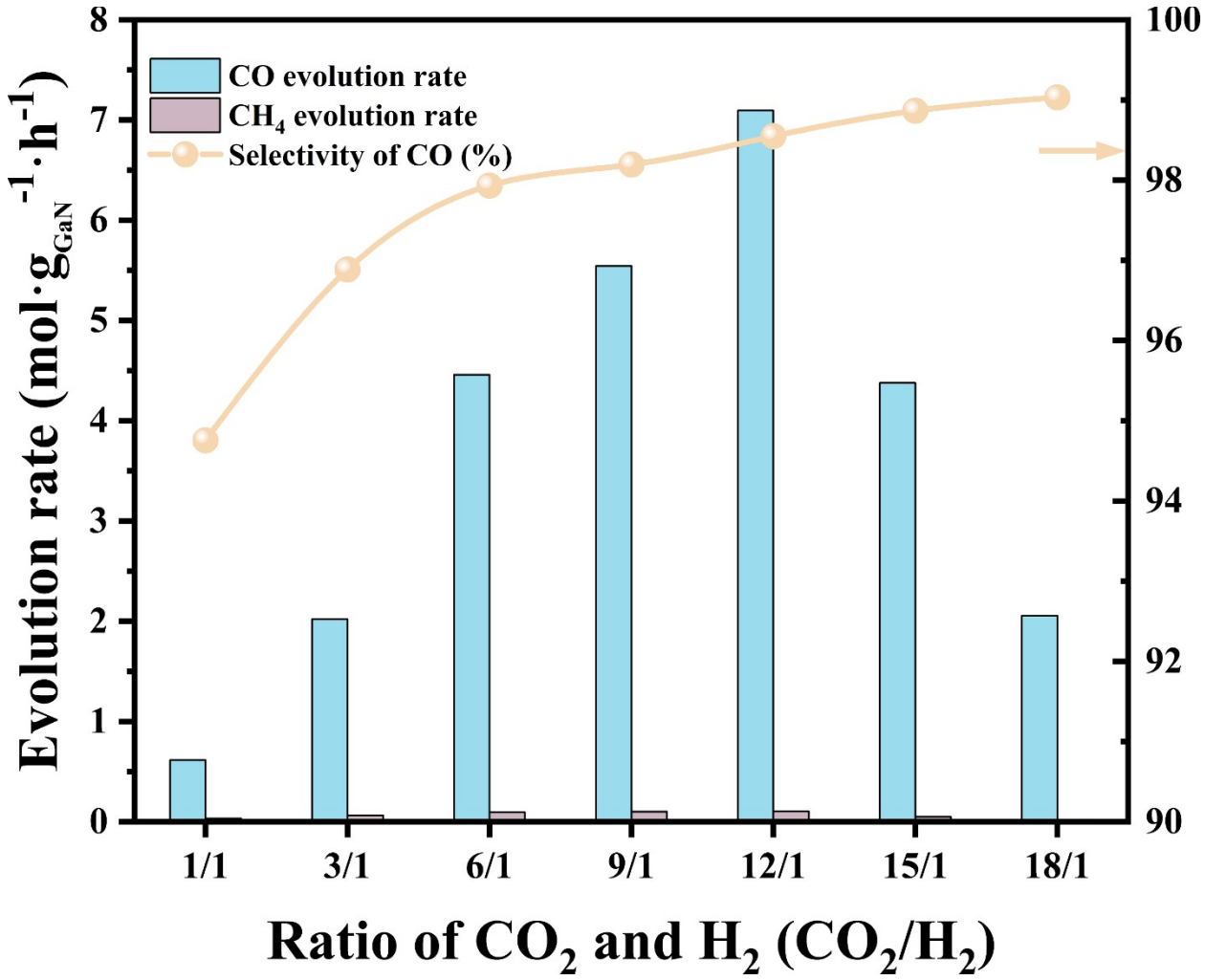

Fig. S18. Influence of CO_2/H_2 ratios on the product evolution rate and selectivity. Light intensity: 4.3 W·cm^{-2}; catalyst area: ~0.5 cm^{-2}; Rh:(Rh + Pt) = 0.55; PtRh; 0.11 μmol·cm^{-2}.

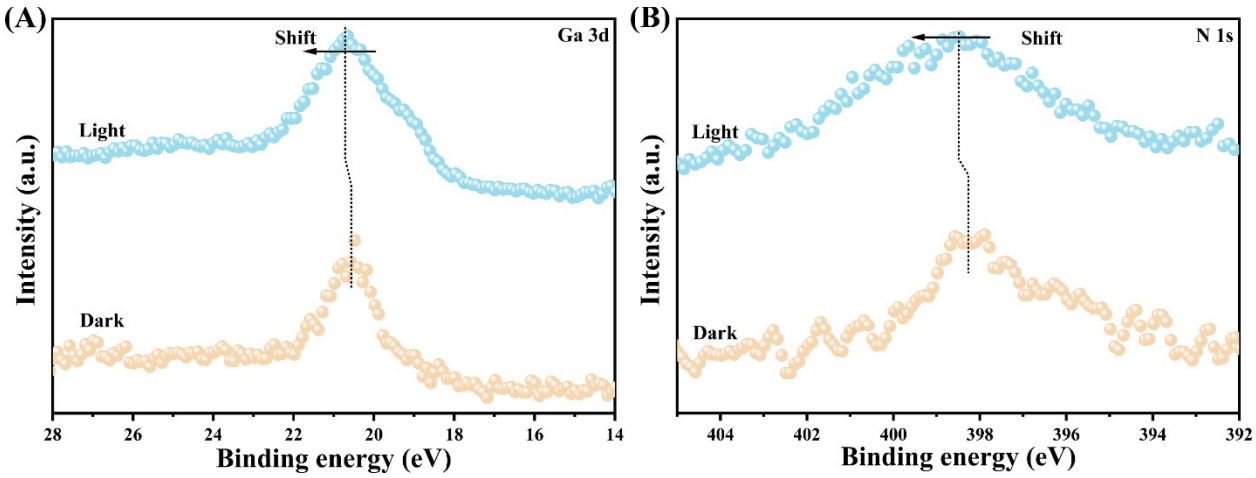

Fig. S19. ISI-XPS spectra of (A) Ga 3d, (B) N 1s.

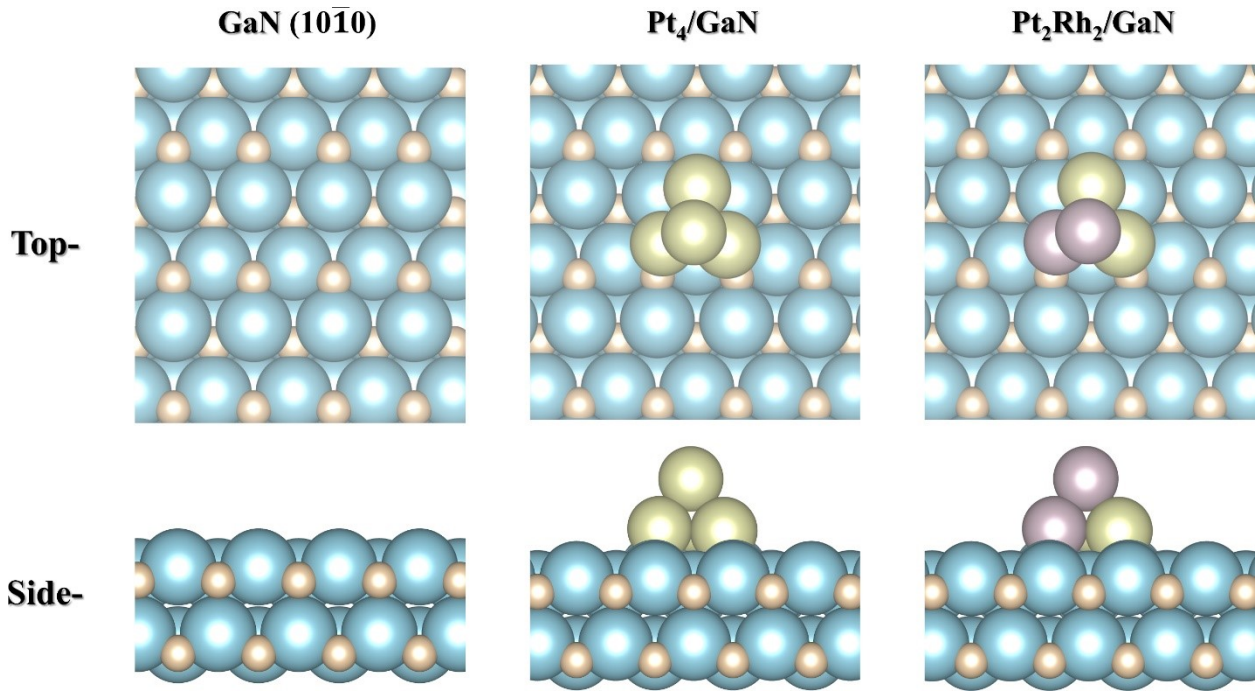

Fig. S20. The top and side views of optimal structural models of GaN (10$\bar{1}$0), Pt_4/GaN, and Pt_2Rh_2/GaN, respectively. Ga, blue; N, orange; Pt, green; and Rh, purple.

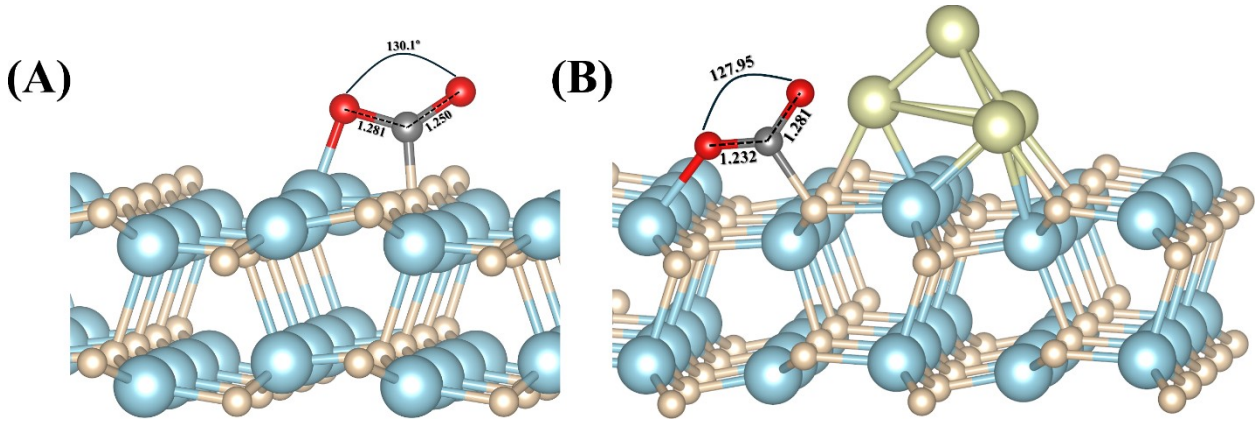

Fig. S21. CO_2 adsorption configuration over GaN ($10\bar{1}0$) and Pt_4/GaN. Ga, blue; N, orange; Pt, green; C, gray; and O, red.

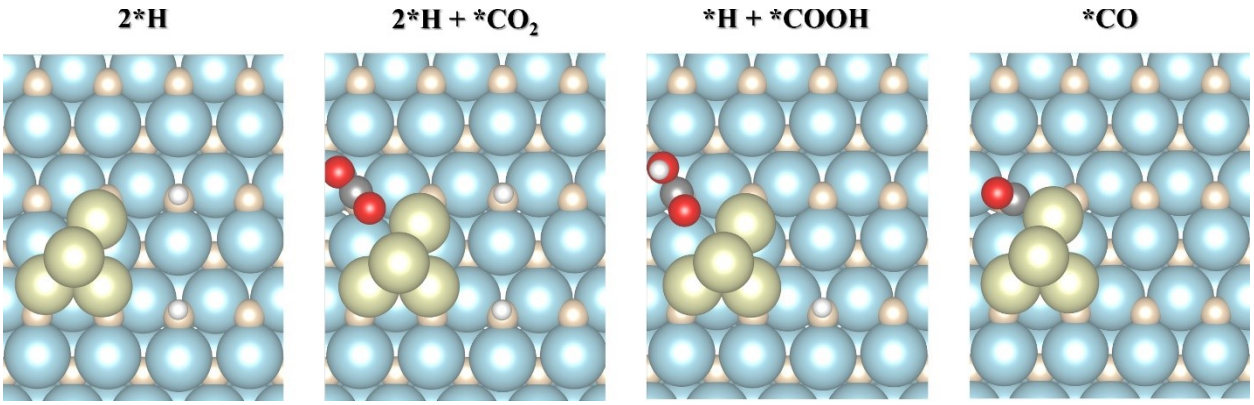

Fig. S22. Optimized geometry of each reaction intermediate for CO_2 hydrogenation on Pt_4/GaN. Ga, blue; N, orange; Pt, green; C, gray; O, red; and H, white.

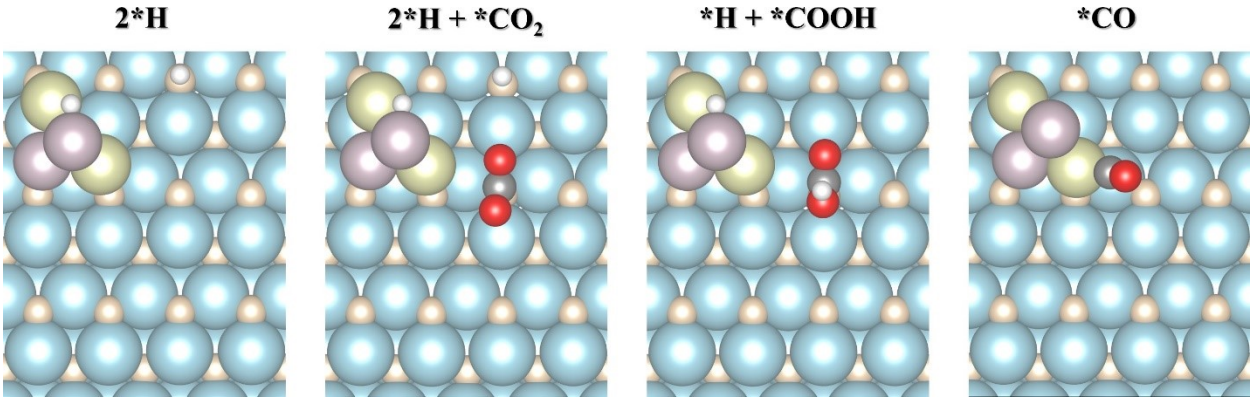

Fig. S23. Optimized geometry of each reaction intermediate for CO_2 hydrogenation on Pt_2Rh_2/GaN. Ga, blue; N, orange; Pt, green; Rh, purple. C, gray; O, red; and H, white.

References

1. J. Ma, J. Yu, G. Chen, Y. Bai, S. Liu, Y. Hu, M. Al‐Mamun, Y. Wang, W. Gong, D. Liu, Y. Li, R. Long, H. Zhao and Y. Xiong, Rational Design of N-Doped Carbon-Coated Cobalt Nanoparticles for Highly Efficient and Durable Photothermal CO_2 Conversion, *Adv. Mater.*, 2023, **35**, 2302537.
2. S. Ning, H. Xu, Y. Qi, L. Song, Q. Zhang, S. Ouyang and J. Ye, Microstructure Induced Thermodynamic and Kinetic Modulation to Enhance CO_2 Photothermal Reduction: A Case of Atomic-Scale Dispersed Co-N Species Anchored Co@C Hybrid, *ACS Catal.*, 2020, **10**, 4726-4736.
3. S. Singh, R. Verma, N. Kaul, J. Sa, A. Punjal, S. Prabhu and V. Polshettiwar, Surface plasmon-enhanced photo-driven CO_2 hydrogenation by hydroxy-terminated nickel nitride nanosheets, *Nat. Commun.*, 2023, **14**, 2551.
4. H. Wang, S. Fu, B. Shang, S. Jeon, Y. Zhong, N. J. Harmon, C. Choi, E. A. Stach and H. Wang, Solar-Driven CO_2 Conversion via Optimized Photothermal Catalysis in a Lotus Pod Structure, *Angew. Chem. Int. Ed.*, 2023, DOI: 10.1002/ange.202305251, e202305251.
5. Z. Wu, J. Shen, C. Li, C. Zhang, K. Feng, Z. Wang, X. Wang, D. M. Meira, M. Cai and D. Zhang, Mo_2TiC_2 MXene-Supported Ru Clusters for Efficient Photothermal Reverse Water-Gas Shift, *ACS Nano*, 2022, **17**, 1550-1559.